Streisinger, G., & Owen, J. (1985) *Genetics 109*, 633–659.
Streisinger, G., Okada, Y., Emrich, J., Newton, J., Tsugita, A., Terzaghi, E., & Inouye, M. (1966) *Cold Spring Harbor Symp. Quant. Biol. 31*, 77–84.
Woodson, S. A., & Crothers, D. M. (1987) *Biochemistry 26*, 904–912.
Young, P. R., & Kallenbach, N. R. (1981) *J. Mol. Biol. 145*, 785–813.

Structural and Dynamic Aspects of Binding of a Prototype Lexitropsin to the Decadeoxyribonucleotide d(CGCAATTGCG)$_2$ Deduced from High-Resolution ^{1}H NMR Studies†

Moses Lee,‡ Ding-Kwo Chang,‡ John A. Hartley,‡ Richard T. Pon,§ Krzysztof Krowicki,‡ and J. William Lown*,‡

Department of Chemistry, University of Alberta, Edmonton, Alberta T6G 2G2, Canada, and Regional DNA Synthesis Laboratory, University of Calgary, Calgary, Alberta T2N 4N1, Canada

Received May 19, 1987; Revised Manuscript Received September 9, 1987

ABSTRACT: Structural and dynamic properties of the self-complementary decadeoxyribonucleotide d(CGCAATTGCG)$_2$ and the interaction between a prototype lexitropsin, or information-reading oligopeptide, and the decadeoxyribonucleotide are deduced by using high-resolution ^{1}H NMR techniques. The nonexchangeable and imino proton resonances of d(CGCAATTGCG)$_2$ have been completely assigned by two-dimensional NMR studies. The decadeoxyribonucleotide exists as a right-handed B-DNA. In the ^{1}H NMR spectrum of the 1:1 complex, the selective chemical shifts and removal of degeneracy of AH2(4), AH2(5), T-CH$_3$(6), and T-CH$_3$(7) due to the anisotropy effects of the heterocyclic moieties of the ligand, and with lesser effects at the flanking base sites C(3) and G(8), locate the drug centrally in the decadeoxyribonucleotide. This conclusion is supported by plots of individual chemical shift changes across the decadeoxyribonucleotide. Similarly, imino protons IV and V experience larger shifts and II and III smaller shifts in accord with this conclusion while drug complexation permits the detection of imino proton I. Strong nuclear Overhauser effects (NOEs) between pyrrole H5 and AH2(5), and weaker NOEs to AH1′(5), TH3′(6), and AH2′(5), firmly locate the ligand in the minor groove. Intraligand NOEs between the adjacent heterocyclic moieties indicate that the lexitropsin is subject to propeller twisting about the N6–C9 bond in both the bound and free forms. Nuclear Overhauser effect spectroscopy (NOESY) and correlated spectroscopy (COSY) experiments also indicate that the removal of degeneracy of the C16 methylene protons upon complexation may arise from restricted rotation about the C15–N9, C15–C16, and C16–C17 bonds. Specific hydrogen bonds between amide NH groups on the concave face of the ligand (N4H, N6H, N9H) and adenine N3 or thymine O2 on the floor of the minor groove are in accord with displacement of the hydration shell by the drug. NOE measurements on the decadeoxyribonucleotide in the 1:1 complex confirm it exists as a right-handed helix and belongs to the B family. Exchange NMR effects permit an estimate of a rate of $\approx$44 s^{-1} for the two-site exchange of the lexitropsin between two equivalent sites on the decamer with $\Delta G^{\ddagger} \approx 70 \pm 5$ kJ mol^{-1} at 294 K. Alternative mechanisms for this exchange process are considered.

The sequence-specific molecular recognition of DNA by proteins is central to the regulation of many biological processes (Caruthers, 1980; Frederick et al., 1984; Gurskii et al., 1977; Kim et al., 1974; Takeda et al., 1983). The oligopeptide antibiotics netropsin and distamycin can serve as models of sequence-specific and groove-selective DNA-binding molecules (Hahn, 1975; Kolchinskii et al., 1975; Kopka et al., 1985; Lown et al., 1986; Patel, 1982; Wartell et al., 1974; Zimmer, 1975; Zimmer et al., 1986). Netropsin and distamycin bind within the minor groove of DNA (Zimmer, 1975) and demand binding sites consisting of (A·T)$_4$ and (A·T)$_5$, respectively. Physical studies including X-ray analysis of a complex of netropsin with the self-complementary dodecamer d(CGCGAATTCGCG)$_2$ (Kopka et al., 1985), ^{1}H NMR investigations (Patel, 1982; Gupta et al., 1984), and circular dichroism (CD) studies (Zimmer, 1975) have provided some structural details on the nature of the interactions between drug and receptor that contribute to their marked specificity. An analysis of these structural requirements for the molecular recognition suggested that replacement of one or more pyrrole groups by hydrogen bond accepting heterocycles such as imidazole should alter this (A·T)$_n$ specificity in a predictable way. This prediction was recently confirmed experimentally, indicating that the imidazole moieties permit the recognition of GC sites by invoking new hydrogen bonds between G–C(2)-NH$_2$ and the imidazole N3 (Lown et al., 1986; Kissinger et al., 1987).

It was clear however that a number of other factors are important determinants of recognition. For example, electrostatic interactions contribute significantly since the marked negative potential wells in the minor groove of (A·T)$_n$ sequences confer a bias for the binding of doubly positively

† This investigation was supported by grants (to J.W.L.) from the National Cancer Institute of Canada and the Biotechnology Strategic Grants Programme of the National Sciences and Engineering Research Council of Canada.
‡ University of Alberta.
§ University of Calgary.

0006-2960/88/0427-0445$01.50/0

Table I: Automated Large-Scale (10–15-μmol) DNA Synthesis Cycle

step no.	step	reagent	time[a]
		Synthesis Cycle	
1	detritylation	3% trichloroacetic acid/dichloroethane	150 s
2	wash	acetonitrile	520 s
3	base addition	0.1 M phosphoramidite + 0.5 M tetrazole/acetonitrile	50 s
4	wait		180 s
5	capping	0.25 M acetic anhydride + 0.25 M (dimethylamino)pyridine/THF[b]	60 s
6	wait		120 s
7	oxidation	0.05 I_2 in THF/pyr/H_2O[b] 7:2:1	210 s
8	wash	acetonitrile	360 s
		Deprotection Cycle	
1		thiophenol/triethylamine/dioxane 1:1:2	30 min
2		15 M ammonium hydroxide	90 min

[a] The times shown are the total times for each operation. Valve block and column flush steps are not shown. Reagent flow rates are approximately 1–2 mL/min. [b] Abbreviations: THF, tetrahydrofuran; pyr, pyridine.

charged ligands. Thus removal of one positive charge in imidazole lexitropsins, or information-reading oligopeptides, permits clean targeting for GC sequences (Kissinger et al., 1987). Additional structural information is required to improve recognition so that structural modification of specificity can proceed in an informed manner. Accordingly, we report the use of high-resolution ^1H NMR techniques to study the structure and dynamics of the decadeoxyribonucleotide d-$(CGCAATTGCG)_2$ and the complex formation between a prototype lexitropsin (Lown et al., 1986) and the decadeoxyribonucleotide.

Materials and Methods

DNA Synthesis—General Methods and Materials. The DNA decadeoxyribonucleotide was synthesized on an Applied Biosystems 380A triple-column DNA synthesizer according to a modified version of the ABI 10-μmol scale synthesis cycle (Table I). N^6-Benzoyl-5′-(dimethoxytrityl)-2′-deoxyadenosine 3′-(*N*,*N*-diisopropylmethylphosphoramidite), N^4-benzoyl-5′-(dimethoxytrityl)-2′-deoxycytidine 3′-(*N*,*N*-diisopropylmethylphosphoramidite), N^2-isobutyryl-5′-(dimethoxytrityl)-2′-deoxyguanosine 3′-(*N*,*N*-diisopropylmethylphosphoramidite), and 5′-(dimethoxytrityl)thymidine 3′-(*N*,*N*-diisopropylmethylphosphoramidite) were synthesized according to previous procedures (Gait, 1984). Long-chain alkylamine controlled-pore glass (Pierce Chemical Co., Rockford, IL) was derivatized for use as the solid-phase support (Gait, 1984). NACS-20 resin was obtained from Bethesda Research Laboratories (Gaithersburg, MD). NACS-20 chromatography was performed with 30 g (dry weight) of resin in a 16 mm × 100 mm glass column along with a Pharmacia P1 peristaltic pump, gradient generator, UV-1 detector, and FRAC-100 fraction collector.

Synthesis and Purification of d(CGCAATTGCG)$_2$. The large-scale synthesis cycle shown in Table I was used with three 15-μmol synthesis columns on the ABI 380A synthesizer. Coupling yields averaged 98–99% as determined by trityl color analysis (Gait, 1984). After completion of the deprotection step by heating (50 °C, 16 h) in 15 M NH_4OH, 2070 OD units of crude material was obtained. Aliquots (400 OD units) of crude material were dried, redissolved in 0.1 M NaCl/12 mM NaOH (1 mL), and applied to the NACS-20 column. The column was eluted first with 0.1 M NaCl/12 mM NaOH (25 mL) and then with the gradient formed between 0.2 M NaCl/12 mM NaOH (275 mL) and 0.4 M NaCl/12 mM NaOH (275 mL), at a flow rate of 1 mL/min. The product eluted with 0.38 M NaCl was collected, and 1.5–2 equiv of 0.5 M aqueous NH_4Cl solution was added to reduce the pH. The combined solutions were then concentrated and dialyzed to yield 700 OD units of oligonucleotide. This was desalted on a Sephadex G-25 column (16 mm × 400 mm) to yield 23 mg (7.1 μmol) of pure oligonucleotide. The homogeneity was ascertained by high-performance liquid chromatography (HPLC) analysis using a C-18 reverse-phase column. After complete digestion of aliquots by *Crotalus durrissus terrificus* snake venom phosphodiesterase, the sample showed the expected nucleoside and nucleotide ratios.

Chemicals. The synthesis and characterization of the oligopeptide [[1-methyl-4-[[1-methyl-4-[(guanidinoacetyl)-amino]pyrrol-2-yl]carboxamido]imidazol-2-yl]carboxamido]propionamidine hydrochloride (**1**) has been reported (Lown et al., 1986; Krowicki & Lown, 1987).

Sample Preparation and NMR Spectroscopy. D_2O (99.8% atom purity) was purchased from General Intermediates of Canada and D_2O (99.996% atom purity) from Aldrich. For the ^1H NMR of the "free" decadeoxyribonucleotide, the sample was prepared by dissolving 20 mg of the decadeoxyribonucleotide in a 99.8% D_2O solution containing 30 mM sodium phosphate and 20 mM sodium chloride at pH 7.1 and then lyophilizing to dryness. The lyophilization was repeated twice more and the sample finally made up to 0.4 mL with 99.996% D_2O. For imino proton NMR studies the sample was dissolved in 9:1 (v/v) H_2O/D_2O solution.

For the 1:1 complex, the sample was prepared by dissolving 8 mg of the decadeoxyribonucleotide and 0.71 mg of **1** in a 99.8% D_2O solution containing 30 mM sodium phosphate, 20 mM sodium chloride, and 1 mM ethylenediaminetetraacetic acid (EDTA) at pH 7.1 and then lyophilizing to dryness. The lyophilization was repeated twice more, and the sample was finally made up to 0.4 mL with 99.996% D_2O. For detection of the exchangeable ^1H NMR signals, the sample was made up in a 9:1 (v/v) H_2O/D_2O solution.

NMR spectra were obtained on Bruker WH400 and WM360 cryospectrometers, both of which were interfaced with Aspect 2000 data systems. The correlated (COSY) and nuclear Overhauser effect (NOESY) spectra were symmetrized but not apodized (Chazin et al., 1986; Marion & Wüthrich, 1983; States et al., 1982). COSY (Aue et al., 1976) and NOESY (Macura & Ernst, 1980; Noggle & Schirmer, 1971) experiments were carried out in the same way as described in our previous studies (Lown et al., 1986).

The $1\bar{3}3\bar{1}$ pulse sequence (Hore, 1983) was used for solvent signal suppression in 90% H_2O solution. In the NOESY experiment the mixing time (0.35 s) was randomly changed by 18% to eliminate spin-coupling effects (Macura & Ernst, 1980). The pulse sequences used for the experiments are as follows: RD (relaxation delay)–$\pi/2$–t_1–$\pi/2$–AQ (acquisition) for COSY and RD–$\pi/2$–t_1–$\pi/2$–τ_m (mixing time)–$\pi/2$–AQ for NOESY.

Thermal Denaturation—UV Hyperchromicity Experiments. The experiments were performed on a Gilford 250 spectrophotometer equipped with a thermal programmer. The buffer solutions used for these experiments consisted of 40 mM sodium phosphate, pH 7.0, and either 0.1 M or 0.5 M sodium chloride.

Results and Discussion

The decadeoxyribonucleotide is numbered d-$(C_1G_2C_3A_4A_5T_6T_7G_8C_9G_{10})_2$ while the five different imino protons are designated by Roman numerals (Figure 1A). The

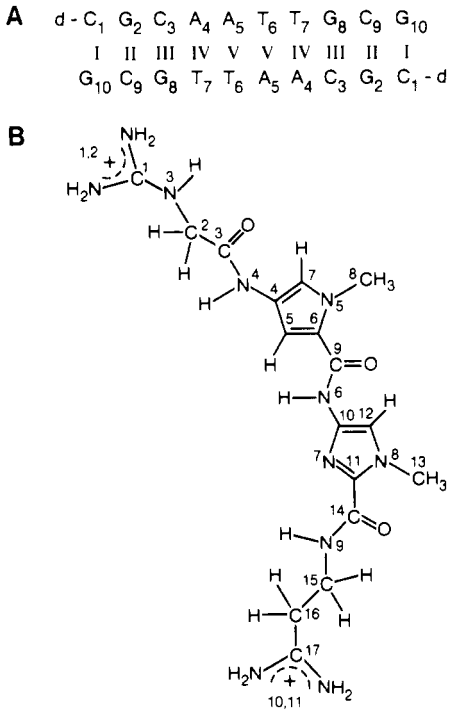

FIGURE 1: Structure and numbering schemes for (A) duplex decamer including imino proton positions and (B) carbons and nitrogens in lexitropsin **1**.

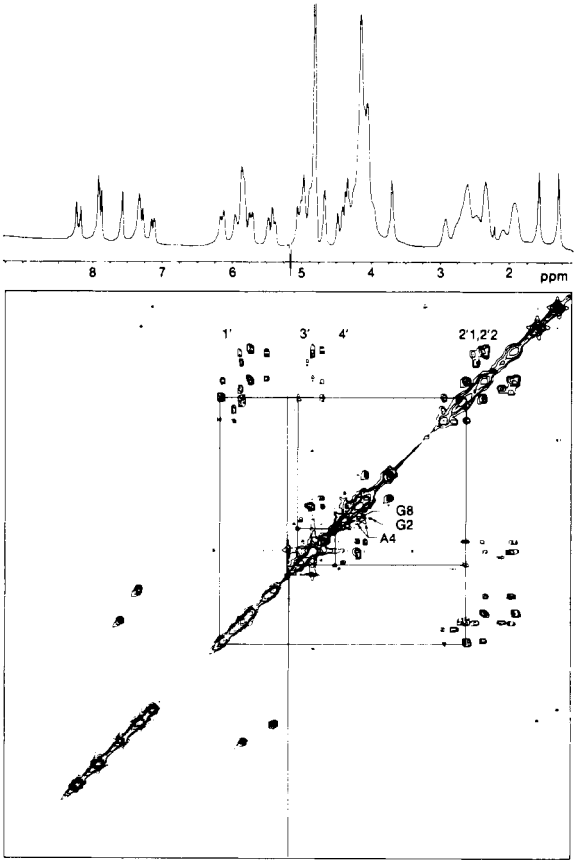

FIGURE 2: COSY-90 contour plot for d(CGCAATTGCG)$_2$ at 21 °C. Experimental conditions: ΔT_1 = 0.3 ms; initial t_1 = 3 μs; 64 free induction decays (FIDs) were accumulated with spectral width = 3300 Hz and $F2$ = 1K for each of 250 experiments.

numbering system for the protons and nitrogens in **1** is adapted from that used in the crystallographic studies on netropsin and is also shown in Figure 1B. The assignment of the chemical shifts of the nonexchangeable protons for the self-complementary decadeoxyribonucleotide follows a similar strategy as that employed for other double-stranded B-form oligonucleotides (Hare et al., 1983). The through-bond connectivities (i.e., protons within the same sugar residue) are established by COSY experiments (Aue et al., 1976; Frechet et al., 1983). In addition, through-space connectivities by dipolar interaction were obtained by NOESY experiments (Macura & Ernst, 1980; Scheek et al., 1983).

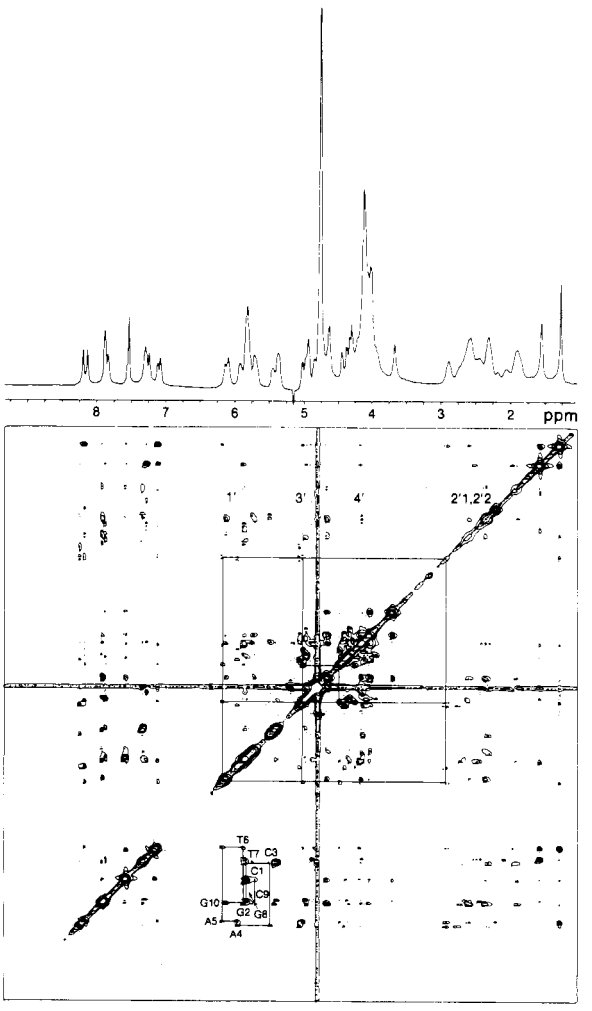

FIGURE 3: NOESY contour plot for d(CGCAATTGCG)$_2$ at 21 °C. Experimental conditions: ΔT_1 = 0.33 ms; spectral width = 3000 Hz; τ_m (mixing time) = 0.35 s; 96 FIDs were accumulated for each of the 340 experiments. The H1′–H8/H6 sequential connectivities are also shown.

^1H NMR Chemical Shift Assignments for d-(CGCAATTGCG)$_2$ at 21 °C. The results for the COSY and NOESY experiments for the decadeoxyribonucleotide are shown in Figures 2 and 3, respectively. The following connectivities were deduced from the COSY and NOESY experiments: (a) 8.26 [AH8(4)]–5.97 [AH1′(4)]–5.05 [AH3′(4)]–4.41 [AH4′(4)]–4.19 [AH5′(4)]–2.92 [AH2′1-(4)]–2.75 [AH2′2(4)]; 8.20 [AH8(5)]–6.17 [AH1′(5)]–5.01 [AH3′(5)]–4.48 [AH4′(5)]–4.26 [AH5′(5)]–2.90 [AH2′1-(5)]–2.59 [AH2′2(5)]. Additional NOESY cross-peaks are observed at 8.26–8.20 and 8.26–7.37 ppm. The doublet at 7.37 ppm can be ascribed to an H6 signal of a cytosine residue from the COSY spectrum (Figure 2), by its correlation to a CH5 proton. It is well documented that adenine H8 protons are located most downfield among all aromatic protons (Lown et al., 1985); therefore, the signals at 8.26 and 8.20 ppm can be assigned to AH8s. Since A(4) is flanked by an adenine and cytosine, the former set of connectivities must belong to A(4).

Table II: Chemical Shifts of Nonexchangeable Protons of $d(CGCAATTGCG)_2$ at 21 °C (in ppm)

base	CH_3	2	8	6	5	1′	2′1	2′2	3′	4′	5′
C1			7.60	5.84	5.73	2.31	1.90	4.68	4.06	3.71	
G2			7.94			5.90	2.70	2.62	4.96	4.35	3.97
C3			7.37	5.45	5.50	2.32	1.92	4.81	4.16		
A4		7.18	8.26			5.97	2.92	2.75	5.05	4.41	4.19
A5		7.59	8.20			6.17	2.90	2.59	5.01	4.48	4.26
T6	1.29		7.13		5.89	2.50	1.97	4.82	4.16		
T7	1.58		7.28		5.88	2.49	2.05	4.90	4.15		
G8			7.88			5.86	2.70				

Imino Proton Assignments for $d(CGCAATTGCG)_2$

I	*a*	12.88[b]
II	12.96	12.96
III	13.71	12.59
IV	13.58	13.69

[a] Not observable at 22 °C because of fraying at termini. [b] Determined at 4 °C.

Saturation of the AH8 signal at 8.20 ppm produced NOE peaks at 1.29 ppm for a thymine methyl group and the AH8(4) signal at 8.20 (also see Figure 3). Therefore, the latter set of connectivities must belong to A(5).

(b) 7.28 [TH6(7)]–5.88 [TH1′(7)]–4.90 [TH3′(7)]–4.15 [TH4′(7)]–2.49 [TH2′(7)]–2.05 [TH2′2(7)]–1.58 [T-C-H_3(7)]; 7.13 [TH6(6)]–5.89 [TH1′(6)]–4.82 [TH3′(6)]–4.16 [TH4′(6)]–2.50 [TH2′1(6)]–1.97 [TH2′2(6)]–1.29 [T-C-H_3(6)]. Since the thymine methyl group at 1.29 ppm has been shown to be close to AH(5), the second of connectivities can be assigned to T(6). Furthermore, the TH6(6) signal is shown to be correlated to the H1′ anomeric proton of A(5) (Figure 3); therefore, as discussed earlier, the duplex is most likely to exist in the B form. The other TH6 signal at 7.28 ppm has additional NOESY correlations to the T-CH_3(6) moiety at 1.29 and to a guanine H8 signal at 7.88 ppm. Accordingly, the first set of connectivities is ascribed to T(7).

(c) 7.95 [GH8(10)]–6.12 [GH1′(10)]–4.68 [GH3′(10)]–4.16 [GH4′(10)]–4.07 [GH5′(10)]–2.59 [GH2′1(10)]–2.35 [GH2′2(10)]; 7.94 [GH8(2)]–5.90 [GH1′(2)]–4.96 [GH3′-(2)]–4.35 [GH4′(2)]–2.70 [GH2′1(2)]–2.62 [GH2′2(2)]; 7.88 [GH8(8)]–5.86 [GH1′(8)]–4.96 [GH3′(8)]–4.37 [GH4′-(8)]–2.70 [GH2′1(8)]–2.45 [GH2′2(8)]. It is well established that the H3′ signal at the 3′ terminal resonates at the highest field among all other H3′ protons (Lown et al., 1985). Since the most upfield H3′ signal is located at 4.68 ppm, one can assign the first set of connectivities to G(10). The signal at 7.94 ppm has NOESY cross-peaks with two CH6 resonances at 7.60 and 7.37 ppm. Since G(2) is positioned between two cytosine residues, the second set of connectivities must belong to G(2). The third set of connectivities can be readily ascribed to G(8) on the basis of an observed NOESY correlation between GH8(8) and TH6(7) at 7.28 ppm (Figure 3).

(d) 7.60 [CH6(1)]–5.84 [CH5(1)]–5.73 [CH′(1)]–4.68 [CH3′(1)]–4.06 [CH4′(1)]–3.71 [CH5′(1)]–2.31 [CH2′1-(1)]–1.90 [CH2′2(1)]; 7.37 [CH6(3)]–5.45 [CH5(3)]–5.50 [CH1′(3)]–4.81 [CH3′(3)]–4.16 [CH4′(3)]–2.32 [CH2′1-(3)]–1.92 [CH2′2(3)]; 7.36 [CH6(8)]–5.39 [CH5(8)]–5.75 [CH1′(9)]–4.81 [CH3′(8)]–4.16 [CH4′(9)]–2.37 [CH2′1-(9)]–1.91 [CH2′2(9)]. From the NOESY spectrum (Figure 3), the CH6(1) signal at 7.60 ppm is correlated to GH8(2) at 7.94 ppm. Furthermore, it is well documented that the protons at the 5′ terminal are found at highest field among all other 5′ hydrogens (Lown et al., 1985). The highest 5′ signal is found at 3.71 ppm; thus, the first set of connectivities is assigned to C(1). From the NOESY spectrum, a weak correlation is observed between 7.37 and 8.26 ppm, suggesting that the second set of connectivities may be ascribed to C(3). Therefore, by the process of elimination, the final set of connectivities can be assigned to C(9). This final assignment is confirmed by the appearance of a NOESY correlation between the CH6(9) signal at 7.36 and the GH8(10) signal at 7.95 ppm.

Saturation of the remaining two aromatic protons, at 7.59 and 7.18 ppm, did not give rise to any nuclear Overhauser effect (NOE) peaks, and on this basis, these two signals are assigned to AH2s of A(4) and A(5). As will be discussed later, the AH2 signals, 7.59 and 7.18 ppm, are assigned to A(5) and A(4), respectively. The assignments of the nonexchangeable protons are summarized in Table II.

The results of the imino proton detection at 21 °C using the $1\bar{3}3\bar{1}$ pulse sequence in 90% H_2O solution (with 10% D_2O for an internal lock signal) are shown in Figure 4. The peak at 13.71 ppm is readily identified as A(4)–T(7) imino resonance IV since an NOE peak at 12.58 ppm is observed when this peak is saturated. The 12.58 ppm peak is therefore attributed to G(3)–C(8) imino resonance III. The imino proton of C(1)–G(10) (resonance I) is not observable presumably owing to the fraying effect prevalent at the conditions employed of room temperature and 20 mM salt. The signal at 13.58 ppm is ascribed to A(5)–T(6) imino signal V, and the 12.96 ppm peak can be identified as G(2)–C(9) imino signal II. The relative chemical shifts of the imino protons are similar to those of the corresponding imino proton signals in $d(CGCGAATTCGCG)_2$ reported by Patel (1982).

The AH2 protons can also be identified by the NOE experiments in which A(4)–T(7)–IV and A(5)–T(6)–V imino protons are saturated. The results indicate that the signals at 7.59 and 7.12 ppm can be assigned to A(5)H2 and A(4)H2 respectively.

However, at 4 °C, the imino proton of C(1)–G(10) (resonance I) is observed at 12.88 ppm in addition to four other resonances: 12.59, 12.96, 13.69, and 13.77 ppm. The assignments of the imino protons are summarized in Table II.

Conformation of $d(CGCAATTGCG)_2$ in Solution. Generally, in B-DNA the pattern of NOE intensities observed is $N_{H2'-H8/H6} \gg N_{H1'-H8/H6} > N_{H3'-H8/H6}$ when the base proton is irradiated (Gronenborn et al., 1985). The other requirement for double-helical DNA of the B family was mentioned earlier, that is, the presence of an NOE between the base proton H8/H6 and the 1′ proton of the 5′ neighbor (Patel et al., 1986; Hare et al., 1983). Saturation of the CH6(1) signal at 7.60 ppm produced NOE signals at 5.97 [–10.6% for CH5(1)], 5.83 (–4.0% for H1′), 2.31 (–6.0% for H2′2), and 1.94 ppm (–10.6% for H2′1). Irradiation of the TH6(7) signal at 7.28 ppm gave NOE peaks at 5.88 (–4.8% for H1′), 2.48 (–13.4% for H2′2), 2.05 (–14.5% for H2′1), and 1.58 ppm [–15.3% for T-CH_3(7)]. When the signal at 7.13 ppm for TH6(6) was saturated, NOE signals at 5.90 (–4.1% for H1′), 2.50 (–5.4% for H2′2), 1.97 (–11.4% for H2′1), and 1.33 ppm [–12.3% for T-CH_3(6)] are

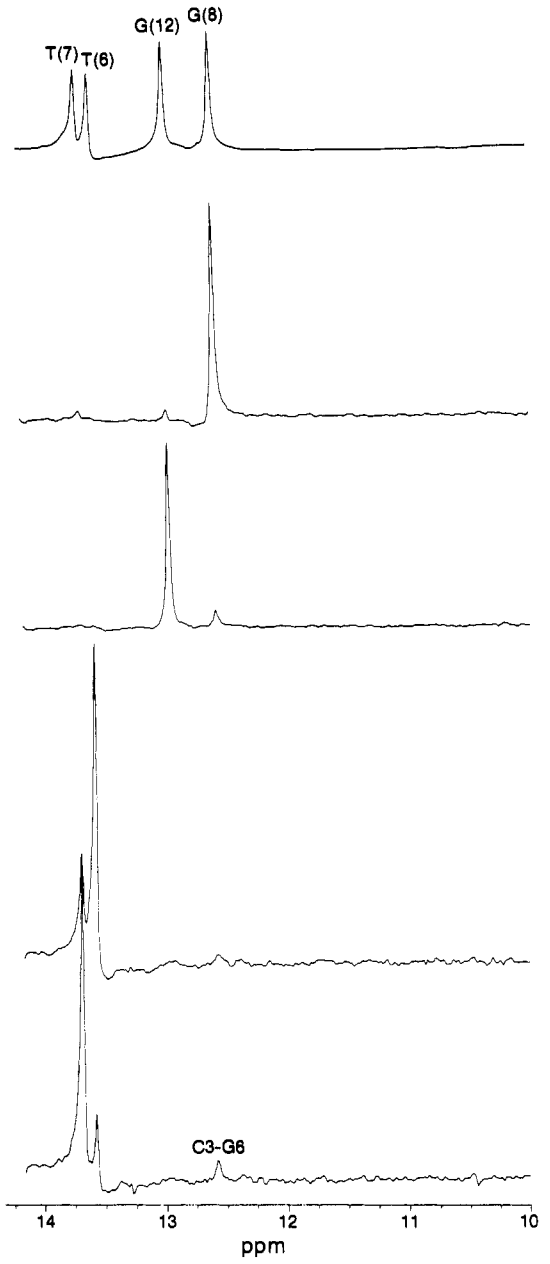

FIGURE 4: 360-MHz imino proton NOE difference spectra at 21 °C. The 1331 pulse sequence was employed to suppress the solvent HOD signal; spectral width = 7200 Hz; irradiation time = 0.95 s; 1600 FIDs were accumulated for each spectrum.

observed. Additional NOE peaks arising from irradiation of TH6(6) are seen at 6.21 [−3.0% for H1′ of A(5)] and 1.58 ppm [−5.0% for T-CH_3(7)]. The observed pattern of NOE intensities for the above three base protons in consistent with that of B-DNA. In addition, the NOE seen between TH6(6) and H1′ of A(5) suggests that this decadeoxyribonucleotide duplex exists in the B form. It is noteworthy that the relatively pronounced NOE between H6/H8 and the 2′1 proton of all bases suggests that the orientation of the base at the glycosyl bond with respect to the sugar moiety is anti and the sugars are in the 2′-endo conformation.

General Characteristics of ^1H NMR Spectrum of the Complex. The spectrum of the nonexchangeable protons of the 1:1 complex of **1** with the decadeoxyribonucleotide is presented in Figure 5 together with the assignment of the aromatic protons. Individual assignments and a comparison with chemical shifts of the components are discussed in the following section (see Table III). In addition to the broadening of individual resonances, binding of the drug destroys the dyad axis of the DNA, and the two strands then give separate NMR resonances. The differences arising from the chemical shift anisotropy (CSA) of the pyrrole and imidazole

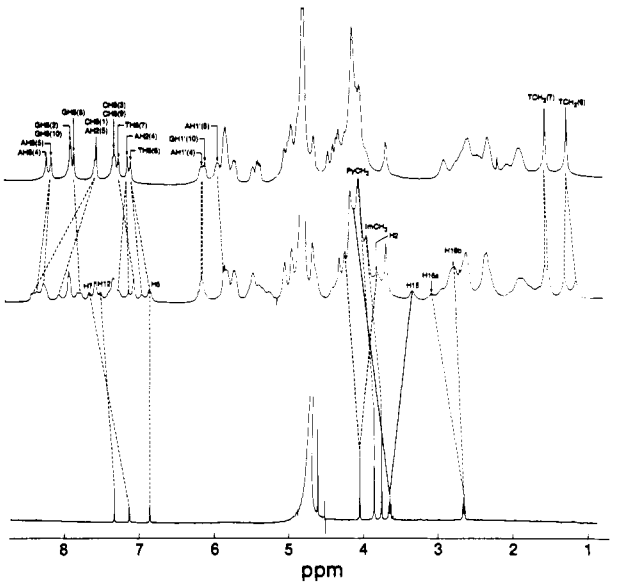

FIGURE 5: One-dimensional ^1H NMR spectra of (top) d-(CGCAATTGCG)$_2$, (middle) 1:1 complex of **1** with decamer, and (bottom) lexitropsin **1**.

Table III: ^1H NMR Chemical Shift Changes (in ppm) of Individual Protons of d(CGCAATTGCG)$_2$ upon 1:1 Complex Formation with Lexitropsin **1** at 21 °C in D_2O Solution

DNA Resonances			
base	DNA	1:1 complex	chemical shift change
CH6(1)	7.60	7.60	0
AH2(4)	7.18	7.18	0
		7.28	+0.10
AH2(5)	7.59	8.08	+0.49
		8.43	+0.84
TH6(6)	7.13	6.98	−0.15
		6.87	−0.26
T-CH_3(6)	1.29	1.32	+0.03
		1.18	−0.11
GH8(8)	7.88	7.84	−0.04
		7.79	−0.09
Imino Protons			
base	DNA	1:1 complex	chemical shift change
C(1)–G(10) I	12.88[a]	13.03	+0.15
G(2)–C(9) II	12.96	12.71	−0.25
C(3)–G(8) III	12.58	12.47	−0.10
A(4)–T(7) IV	13.71	14.18	+0.46
		14.02	+0.30
A(5)–T(6) V	13.58	13.85	+0.28
		13.53	−0.04
Lexitropsin Resonances			
position	free drug	1:1 complex	chemical shift difference
H2	4.15	3.86	+0.29
		4.20	−0.05
Py-H5	6.94	6.86	+0.08
Py-H7	7.20	7.67	−0.47
Py-CH_3	3.97	4.03	−0.06
Im-H12	7.40	7.53	−0.13
Im-CH_3	3.86	3.97	−0.11
H15	2.78	2.83	−0.05
		3.09	−0.31
H16	3.74	3.35	+0.39
		4.08	−0.34

[a] Recorded at 4 °C.

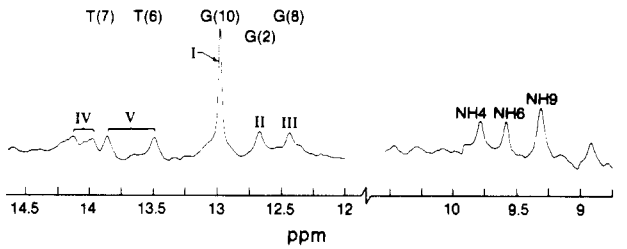

FIGURE 6: DNA imino proton and **1** amide proton spectrum of 1:1 **1**–d(CGCAATTGCG)$_2$ complex in 90% H_2O solution at 21 °C. The spectrum was obtained by applying the 1331 pulse sequence to suppress the solvent signal.

rings is sufficiently large to split the resonances of AH2(4), AH2(5), T-CH_3(6), TCH_3(7), and even GH8(8) as well as the imino protons of T(6) and T(7) (Figure 6). During this process the chemical shift of GH8(10) and CH6(1) of the terminal residues remains essentially unchanged. These results suggest that the lexitropsin is located on the AATT sequence of the DNA.

DNA Imino Protons and Location of Lexitropsin on the Sequence. Similar selective effects are noted with the imino proton resonances (Figure 6). Thus, while the peaks of the T(6) and T(7) imino protons experience significant chemical shift changes, and G(2) and G(8) imino proton resonances experience relatively smaller changes upon complex formation (see Table III). These data are consistent with the binding of the drug in the minor groove of the DNA duplex. A broad peak appears at 13.03 ppm which has a greater intensity than those of the other guanine imino proton peaks or that in the free decamer. The terminal fraying is apparently reduced or the exchange of the terminal imino proton is apparently slowed down by the binding of the drug. This conclusion is supported by independent electron microscopy studies of the oligopeptide antibiotic netropsin to pBR322 singly cut with *Hind*III where enhanced annealing of the "sticky ends" is observed upon binding of the drug to form linear aggregates (J. W. Lown and J. A. Hartley, unpublished work).

The mode of binding of **1** to the decadeoxyribonucleotide is further elucidated by one-dimensional (1D) NOE studies. The assignment of the two imino proton V signals is verified by the large NOE peak at 13.85 ppm when the 13.53 ppm peak is saturated, and vice versa. In addition, saturation of imino proton IV also results in NOE signals at 9.31 ppm for NH9 and at 6.86 ppm for pyrrole H5. These data are consistent with the binding of the drug at the AATT site in the minor groove of the DNA, as shown in Figure 7.

Geometry of Lexitropsin within the Complex. Several exchangeable proton peaks are detected at 9.31, 9.59, and 9.80 ppm in the **1**–decadeoxyribonucleotide complex at 21 °C (Figure 6). These may be ascribed to the amide proton resonance of the drug due to hydrogen bond formation in the minor groove of the DNA, and they are not observable in the NMR spectrum of the free drug.

The concave surface of lexitropsin **1** is lined with alternating pyrrole and amide protons in the sequence CH_2, NH4, CH5, NH6, and NH9. Complexation of the concave face of **1** to the minor groove at the AATT site of the duplex decadeoxyribonucleotide could position these protons close to AH2(4) and AH2(5) of the DNA. Thus one would predict NOEs among these concave face protons and between them and DNA minor groove protons. Saturation of AH2(4) signals at 7.18 and 7.28 ppm produces weak NOE peaks at 6.86, 4.20, and 3.86 ppm for H5 of the pyrrole ring and H2a and H2b of drug. Furthermore, saturation of pyrrole H5 gave strong NOE signals at 8.43 and 8.08 ppm for AH2(5) and weak

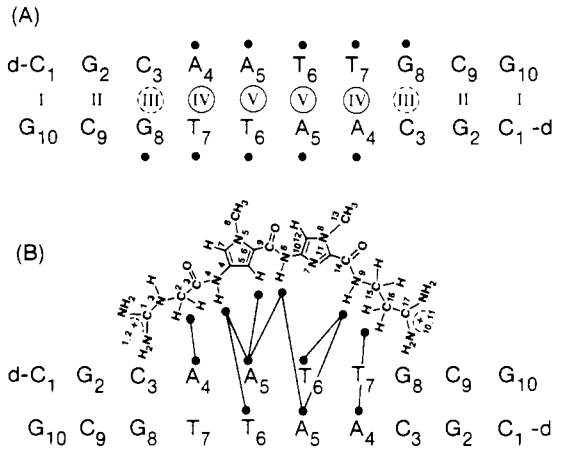

FIGURE 7: (A) Selective chemical shift anisotropy effects resulting from lexitropsin binding and producing (open circles) doubling of proton resonances and (dashed-outline circles) broadening of signals. Filled circles represent protons involved in intermolecular NOEs. Because binding of the lexitropsin removes the symmetry of the DNA, a second identical structure can be drawn. (B) Alignment of **1** relative to the duplex decadeoxyribonucleotide deduced from NOE experiments.

FIGURE 8: One-dimensional ^1H and ^1H NOE difference spectra of 1:1 **1**–d(CGCAATTGCG)$_2$ in D_2O at 21 °C. Spectral width = 3600 Hz; irradiation time for NOE experiment = 0.4 s. The arrows indicate the peaks that are irradiated, and asterisks show the NOEs observed.

signals at 7.28 ppm for AH2(4) (Figure 8B).

The three amide protons on the concave face of **1** in the drug–DNA complex (Figure 7B) were assigned on the basis of the data given below. When the amide proton at 9.50 ppm was irradiated, NOEs to the two other amide protons were observed and therefore must be assigned to NH6 which is located between NH4 and NH9. In addition, a weak NOE was also observed at 8.08 ppm for AH2(5). Saturation of the

amide NH signal at 9.80 ppm results in weak NOE peaks at 9.50 ppm for NH6 and at 6.86 ppm for pyrrole H5. When the remaining 9.31 ppm amide proton was irradiated, weak NOEs at 9.50 ppm for NH6 and 8.43 and 8.08 ppm for AH2(5) were seen. These results permit assignment of the 9.80 and 9.31 ppm resonances to the NH4 and NH9 amine protons, respectively. It should be noted that there are NOEs between the concave face amide protons and pyrrole H5 and AH2(5) but negligible NOEs between these concave face protons and AH2(4). These data require that the drug binds in the minor groove at the AATT site close to AH2(5), as depicted in Figure 7B.

The convex face protons (H7, H12, Py-CH_3, Im-CH_3) of lexitropsin **1** bound to the DNA were assigned on the basis of the data given below. Saturation of the concave pyrrole H5 signal produces not only NOEs as mentioned above but also NOEs to the convex pyrrole H7 and imidazole H12 protons (Figure 8A,D), at 7.67 and 7.53 ppm, respectively. In addition, irradiation of the H7 and H12 signals produces NOE signals at 4.03 and 3.97 ppm for Py-CH_3 and Im-CH_3, respectively. The signals for Py-CH_3 and Im-CH_3 in the free drug resonate at 3.97 and 3.86 ppm, respectively.

The above-mentioned NOE between pyrrole H5 and imidazole H12 of the drug–DNA complex implies that the two protons must be in close proximity; thus the heterocyclic rings cannot be coplanar, as they are in the netropsin–d(CGCGAATTCGCG)$_2$ complex in the crystalline state (Kopka et al., 1985). A possible explanation for this observation is "propeller twisting" along the N6–C9 amide bond, thereby bringing the H5 and H12 protons closer together. If the two rings were coplanar, the distance between H5 and H12 is about 9.6 Å, and no NOE would be observed. If one assumes that the NOE buildup is still in the linear phase during the 0.4-s irradiation time used (Gronenborn et al., 1985), the distance between pyrrole H5 and imidazole H12 can be estimated (Patel et al., 1983). The measured cross-relaxation rate (product of the steady-state NOE of H12 when H5 was irradiated and the spin–lattice relaxation, 1.0 s for imidazole H12) can be used to derive the interproton distance between H5 and H12 of about 4.2 Å at 21 °C. Recent theoretical studies (Zakrzewska et al., 1983) and X-ray analysis (Berman et al., 1979) of netropsin revealed that it adopts a nearly coplanar conformation under these conditions. However, we found that free lexitropsin **1**, an imidazole-containing analogue of netropsin, also exists in the propeller-twisted conformation in D_2O solution at 21 °C, similar to its conformation within the 1:1 drug–DNA complex. This is established by the appearance of an NOE signal for Im-CH_3 at 3.86 ppm when the Py-CH_3 signal at 3.97 ppm was saturated. The presence of an NOE signal between Py-CH_3 and Im-CH_3 is only possible if the two heterocycles in **1** are not coplanar, i.e., if they are twisted. The distance between the two Py-CH_3 groups in coplanar netropsin is about 10.7 Å. The chemical shift for Py-CH_3 is secured on the basis of an additional weak NOE peak at 7.20 ppm (narrow doublet) for the convex pyrrole H7, when the signal at 3.86 ppm is saturated.

Assignment of Nonexchangeable Protons in the **1***–DNA Complex.* The assignment of the ^{1}H NMR resonances of the drug protons and the base protons of the DNA were made by using 1D NOE experiments (Figure 8), COSY (Figure 9), and NOESY (Figure 10), which also permitted the location of the drug binding site in the DNA.

The principal assignments thereby deduced are presented in Figure 5. The peak at 6.86 ppm can be assigned to H5 of the pyrrole ring since the intensity of this peak increases with

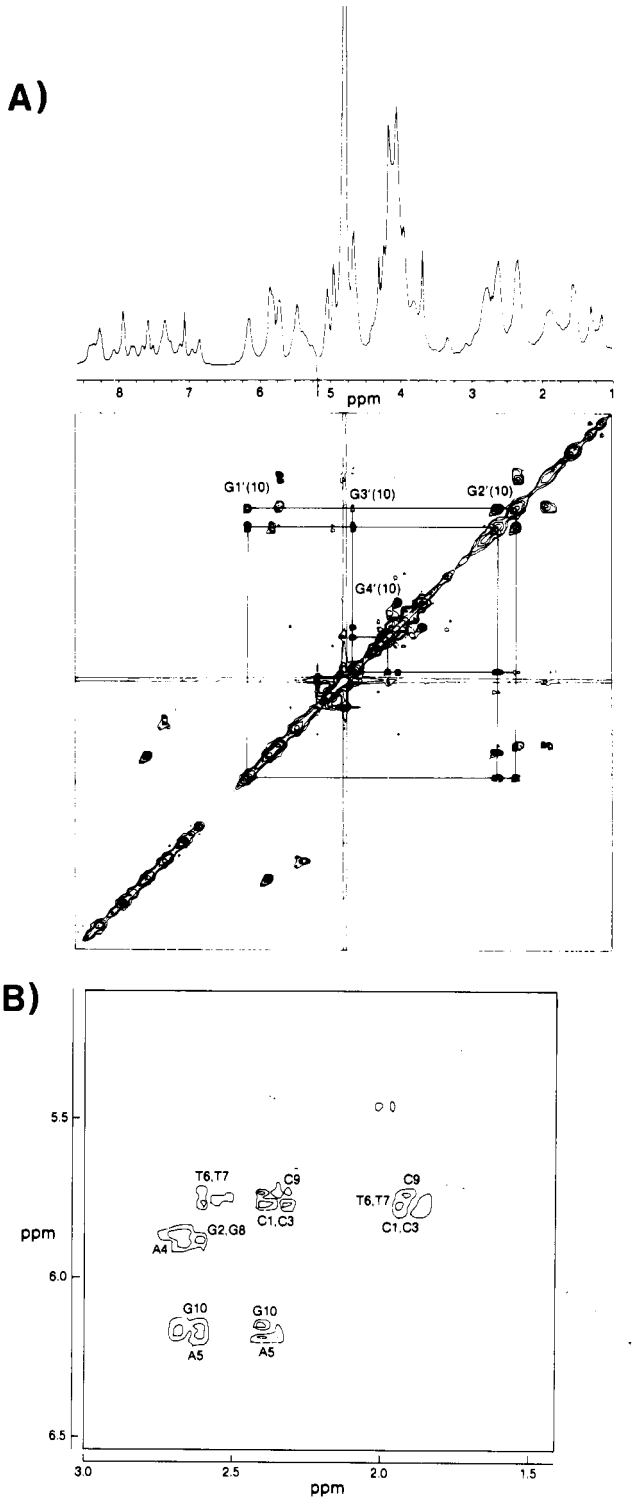

FIGURE 9: (A) COSY-90 contour plot of 1:1 **1**–d(CGCAATTGCG)$_2$ at 21 °C. Experimental conditions: initial t_1 = 3 μs; Δt_1 = 0.28 ms; spectral width = 3600 Hz; 64 FIDs were accumulated for each of the 256 experiments. (B) Expansion of COSY spectrum of 1:1 **1**–decamer complex from 3.00 to 1.41 ppm.

titration of the drug (data not shown). This signal is shifted 0.07 ppm upfield compared with the free drug. Saturation of this peak results in NOE peaks at 8.43 and 8.08 ppm. These two peaks can be identified as AH2(5) (Figure 8B). The degeneracy of the AH2 protons is removed by the anisotropy effects of the pyrrole and imidazole rings, and it is evident that the binding site is at the central AATT core of the DNA. The assignment of the two AH2 protons was verified by the large NOE peak at 8.43 ppm when the 8.08 ppm peak is saturated

Table IV: Chemical Shift Changes upon Complexation

DNA	5′-C_1 G_{10}	G_2 C_9	C_3 G_8	A_4 T_7	A_5 T_6	T_6 A_5	T_7 A_4	G_8 C_3	C_9 G_2	G_{10}-3′ C_1-5′
imino ^{1}H	+0.15	−0.25	−0.10	0.46	0.28	0.04	0.30	−0.10	−0.25	0.15
H6, H8 (av)	0	0	0.07	0.08	0.14	−0.21	−0.10	−0.07	0	0
H2′1	0.06	−0.02	0.03	−0.26	−0.23	0.16	0.20	−0.02	−0.05	0.01

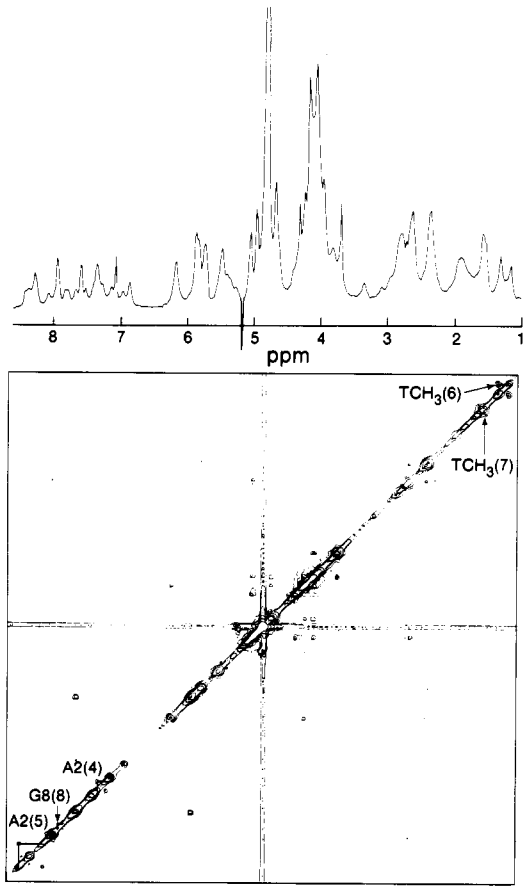

FIGURE 10: NOESY contour plot of 1:1 **1**–d(CGCAATTGCG)$_2$ at 21 °C. Experimental conditions: initial t_1 = 3 μs; Δt_1 = 0.28 ms; mixing time = 0.15 s; spectral width = 3600 Hz; 96 FIDs were accumulated for each of 256 experiments.

and vice versa (Figure 8C,E). The large NOE at 7.28 ppm resulting from irradiation at 7.18 ppm and vice versa leads to the assignment of these two peaks to AH2(4). The significant NOE peaks at 8.43 and 8.08 ppm, but not at 7.28 and 7.18 ppm by irradiation of the pyrrole H5 peak, indicates that the pyrrole ring is bound to the central residues of the DNA duplex. The splitting of the TH6(6) resonance upon complexation into 6.98 and 6.87 ppm is deduced from the strong NOE peak at 6.98 ppm upon saturation of the 6.87 peak or vice versa (Figure 8F). The splitting of the AH8(5) resonance into 8.38 and 8.29 ppm was deduced in a similar fashion (Figure 8G).

An upfield shift of 0.10 ppm is observed upon complex formation for the TH6(7) resonance at 7.13 ppm. By contrast, only very small chemical shift changes can be detected for AH8(4), GH8(2), GH8(10), CH6(1), CH6(3), or CH6(9) (Table III). However, the GH8(8) peaks appear to be close to the onset of coalescence of split peaks, the separation of which is about 0.04 ppm. The conclusion that G(8) and C(3) are on the periphery of the drug binding site is in accord with the results on the imino proton signals discussed above.

It has been demonstrated that the COSY cross-peak for cytidine CH5–CH6 in oligonucleotides is sensitive to the local environment and mobility of the oligomer, and upon drug binding to the cytidine residue, the intensity of the cross-peak is reduced (Borah et al., 1985). Three CH5–CH6 correlations are seen in the COSY spectrum of the free decamer (Figure 1) and its 1:1 drug–DNA complex (Figure 9A). The lower field cross-peak is assigned to C(1), and the overlapping higher field cross-peaks are due to C(3) and C(9). By comparison of the intensities of the CH5–CH6 cross-peaks in the free DNA and the drug–DNA complex, the change in intensity for C(1) is minimal, but the intensity for the overlapping C(3) and C(9) cross-peaks is reduced. It is not possible to determine which of these two cytidine residues [C(3) or C(9)] is involved in binding to the drug by this method; however, as will be discussed below, it seems most likely that C(3) is involved in the binding process.

NOE and COSY (Figure 9) experiments indicate that the resonances at 4.08, 3.35, 3.09, and 2.83 ppm are coupled. By comparison with those in the free drug spectrum the peaks at 4.08 and 3.84 ppm are assigned to the methylene protons at C15 and those at 3.09 and 2.83 ppm to the methylene protons at C16. The splitting of these latter signals is probably due to the restricted rotation of the C15–N9, C15–C16, or C16–C17 bonds upon binding to DNA, or else it reflects their exposure to the dissymmetric environment of the minor groove of the duplex.

The most direct evidence for binding of **1** to the minor groove of the DNA is the strong NOE observed between H5 of the pyrrole moiety and AH2(5). Weak NOE peaks are also observed for AH1′(5) (6.15 ppm), TH3′(6) (4.63 ppm), and AH2′(5) (2.80 ppm). This also supports a binding mode in which the two aromatic rings of the drug are situated close to the central residues of the DNA decamer. The drug–DNA interaction specificity is enhanced by the hydrogen bond formation between amide positions NH4, NH6, and NH9 of the drug and adenine N3 or thymine O2 of the DNA molecule. These latter interactions were detected from the ^{1}H resonances at 9.31, 9.50, and 9.80 ppm of the complex in H_2O solution. The results suggest the exclusion of the sheath of water molecules from the floor of the minor groove as in the case of netropsin (Kopka et al., 1985).

Weak NOE peaks at 4.20 and 3.86 ppm are induced as AH2(4) at 7.18 or 7.28 ppm is irradiated, leading to the assignment of peaks at 4.20 (Figure 8E) and 3.86 ppm to the methylene protons of C2 of **1**. This interaction is also in agreement with the binding mode given in Figure 7. The peak at 7.53 ppm can also be identified as H12 of the imidazole ring since saturation of this peak induces a marked NOE peak at 3.97 ppm which is due to the N–CH_3 group of the imidazole ring. The latter group resonates at 3.86 ppm in the free drug. Similarly, saturation of the peak at 7.67 ppm generates an NOE peak at 4.03 ppm (Figure 8H). These two peaks are assigned to H7 and NCH_3 of the pyrrole ring, respectively. An NOE peak at 3.35 ppm is generated upon saturation of the H12 of the imidazole ring at 7.53 ppm.

In Figure 11, the drug-induced changes in the chemical shifts of selected protons (also see Table IV) of the DNA duplex are plotted versus the sequence. These graphs demonstrates that lexitropsin **1** strongly influences the chemical shifts of the nucleotides A(4) to T(7) and weakly influences G(8) and C(3). Since the base protons TH6(6) and GH8(8)

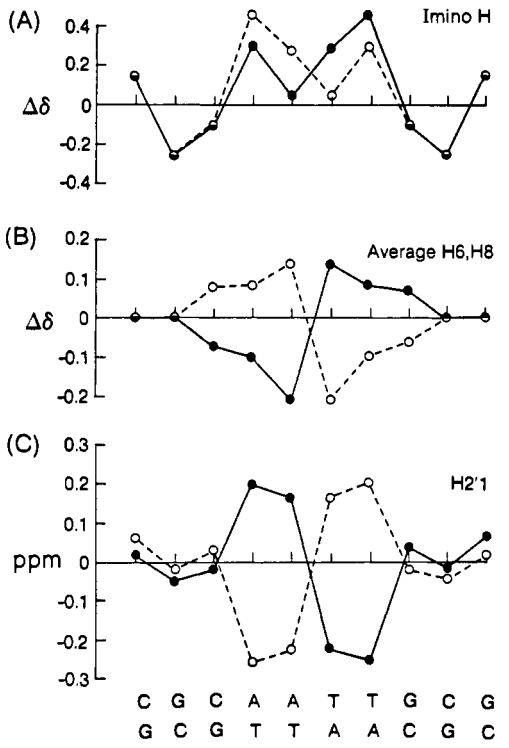

FIGURE 11: Graphical presentation of drug-induced chemical shift changes for selected protons in the DNA sequence. Positive values indicate that the resonances in the complex are at lower field than in the free DNA duplex. The complementary strands of the DNA are shown at the bottom, and the drug-induced chemical shift graphs for each of the two strands are drawn.

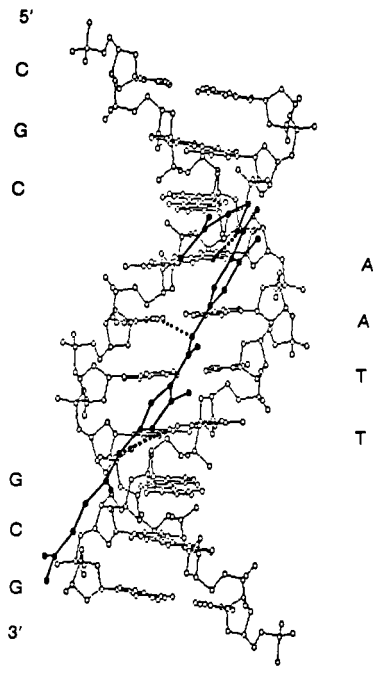

FIGURE 12: Computer-generated depiction of lextropsin **1**–d-(CGCAATTGCG)$_2$ complex. The dotted lines indicate the hydrogen bonds between ligand and DNA.

are split due to slow exchange, averages of the two individual exchanging signals are used in Figure 9B. Overall, the chemical shift measurements thus indicate that drug **1** binds predominantly to the minor groove [A(4)A(5)T(6)T(7)]$_2$ segment in the DNA duplex. These nucleic acid chemical shifts cannot be interpreted in a straightforward manner since they arise from a combination of the magnetic anisotropy of the pyrrole and amide functional groups, as well as from conformational changes in the DNA associated with complex formation. There does not appear to be a pattern to these changes since for the same type of proton we detect a large shift for the imino proton of A(4)–T(7) compared to A(5)–T(6) (Figure 11A) but the reverse is true for AH8 protons for the same base pairs in the complex (Figure 11B).

Studies of the related oligopeptide agents netropsin to d-(GGAATTCC)$_2$ (Patel et al., 1986a) and of distamycin to d(CGCGAATTCGCG)$_2$ (Klevit et al., 1986) have been reported. The conclusions regarding the binding sites on the DNA are in agreement with the present results.

Melting Temperature Studies of 1:1 Complex of **1**–*Decadeoxynucleotide by Determination of UV Hyperchromicity.* The UV optical density change at 260 nm was monitored while the complex underwent thermal denaturation. The results of the UV absorption change with temperature for the self-complementary decamer and the 1:1 **1**–decadeoxyribonucleotide compelx in 40 mM sodium phosphate/0.1 M NaCl at pH 7.1. The **1**–decadeoxyribonucleotide solution exhibits a sharp increase in absorbance with increasing temperature with pronounced T_M = 60 °C under these conditions. The curve for the decadeoxyribonucleotide alone shows only a broad melting behavior. This suggests that the duplex DNA is considerably stabilized by minor groove binding with **1**. The interaction of this lexitropsin with DNA was further examined at higher ionic strength conditions. Thermal denaturation on hyperchromicity of the 1:1 complex in the medium 40 mM sodium phosphate/0.5 M NaCl at pH 7.1 was also examined. The helix to coil transitions are sharper owing to increased stabilization of the DNA duplex by the higher salt concentrations. The measured T_M's are 55.5 and 61 °C for the DNA and **1**–DNA, respectively. The stabilization afforded by binding of the lexitropsin correlates well with the observation of the terminal imino proton at 21 °C in the drug–DNA complex solutions because of the reduced fraying effect and thus reduced exchange rate with the solvent.

Conformation of DNA in Drug–DNA Complex. As mentioned above, in B-DNA, the pattern of NOE intensities observed is $N_{H2'-H6/H8} \gg N_{H1'-H6/H8} \gtrsim N_{H3'-H6/H8}$ when the base proton is saturated (Gronenborn et al., 1985). Furthermore, in a right-handed DNA helix, an NOE peak should be observed between the base proton (H6 of pyrimidine and H8 of purine) and the anomeric 1′ proton of the 5′ neighbor (Patel et al., 1986; Hare et al., 1983). When the TH6(7) signal at 7.08 ppm was irradiated, NOE peaks at 5.30 (–10.0% for H1′), 4.73 (–11.0% for H3′), 2.68 (–21.8% for H2′2), 1.78 (–27.6% for H2′2), 1.58 [–29.3% for T-CH_3(7)], and 5.40 ppm [–2% H1′ of T(6)] are observed. As another example, saturation of the CH6(1) peak at 7.60 ppm results in NOE signals at 5.85 (–14.1% for CH5), 5.75 (–2.5% for H1′), 4.67 (–1.0% for H3′), 2.39 (–3.0% for H2′2), and 1.91 ppm (–12.8% for H2′1). The observed pattern of NOE intensities of H1′, H2′, and H3′ for a given nucleotide, when the base proton is irradiated, is consistent with that of B-DNA. Furthermore, the NOEs observed between TH6(7) and H1′ of T(6) and between TH6(6) and H1′ of A(5) indicate that the duplex exists in the right-handed form. The DNA in the complex exists as a right-handed helix of the B family and is very similar in its conformation to that of the free decadeoxyribonucleotide.

Figure 12 shows a computer-generated diagram of the 1:1 **1**–d(CGCAATTGCG)$_2$ complex; it is seen that lexitropsin **1** fits snugly in the minor groove. Four base pairs of the sequence [A(4)–T(7)] are hydrogen bonded to **1**, as indicated by the dotted line (···). The intermolecular contacts for the **1**–AATT decamer complex in solution (Figure 12) are generally in good

agreement with those of the 1:1 netropsin–d-$(CGCGAATTCGCG)_2$ complex in solution (Patel, 1982), except in the former case, the drug moiety **1** of the complex is propeller twisted.

Dynamics of Lexitropsin–DNA Complex Formation in Solution. The chemical exchange cross-peaks at 7.18–7.28, 8.08–8.43, 1.32–1.18, 7.84–7.79, and 8.38–8.29 ppm are indicative of the dynamic equilibrium of the drug in the complex (Figure 7). It is possible to deduce the exchange rate of the lexitropsin between the two equivalent sites on the decamer. The chemical shift differences arise from the intrinsic dissymmetry of the drug bound to the sequence. The onset of coalescence for GH8(8) and T-CH_3(7) signals at 294 K can be used to estimate the exchange rate of **1** between different binding sites from the standard formula reported by Sutherland (1971):

$$K_{coal} = (\pi/2^{1/2})\Delta\nu = 2.22\Delta\nu \qquad (1)$$

In both the GH8(8) and T-CH_3(7) signals, $\Delta\nu$ values are about 20 Hz; therefore, the rates of exchange of **1** between different binding sites are estimated to be $\approx 44\ s^{-1}$ at 294 K.

From eq 2 (Günther, 1980), an estimate of the activation energy for the observed exchange process at the coalescence temperature T_{coal} can be made. This equation is based on

$$\Delta G^{\ddagger} = 19.14T_{coal}[9.97 + \log (T_{coal}/\Delta\nu)]\ (J\ mol^{-1}) \qquad (2)$$

transition-state theory. From the coalescence involving GH8(8) and T-CH_3(7) (T_{coal} = 294 K), $\Delta G^{\ddagger}$ for both signals of 70 ± 5 kJ mol^{-1} are calculated. The identical activation energy values suggest that the two observed coalescence phenomena are due to the same exchange process.

Alternative Exchange Mechanisms for the Lexitropsin–Decamer Complex. Possible alternative mechanisms for the two-site exchange process for the lexitropsin–decadeoxyribonucleotide complex to be considered include intermolecular exchange between neighboring DNA molecules, intramolecular sliding, "walking" of the ligand, and flip-flop of the drug against the DNA sequence. The recognition sequence of the lexitropsin is the central AATT core (Figure 13), and the regions of the DNA that are subject to selective chemical shift anisotropy effects as a result of drug binding are restricted to the sequence CAATTG (shaded in Figure 13). This loss of degeneracy (i.e., doubling of resonances) can only arise as a result of drug binding wherein the two strands now have separate identities. In contrast, when the drug binds to the DNA, the signals from the heterocyclic bases show only a single set of signals and the only signals to be doubled are those of the prochiral methylene groups at C2, C15, and C16 as a result of their residence in a chiral environment. Thus the exchange process does not result in a change in chemical environments for the drug molecules. It would appear then that a sliding mechanism (Figure 13A) is unlikely since this would result in distinct changes in the chemical environment for the drug during the exchange process, although it is just conceivable since minor chemical shift changes are observed to C(3)–G(8) and G(8)–C(3) positions. Similarly, a walking mechanism represented by Figure 13B, which has been considered for bisintercalative binding (LePecq et al., 1967), may be rejected by the symmetry and chemical shift arguments.

Instead, a flip-flop mechanism is the simplest model to fit the data. As has been pointed out by Klevit et al. (1986), this can be represented by a first-order exchange mechanism in which the drug molecule remains loosely associated with the DNA but rearranges to become associated with the opposite strand of the DNA molecule. The flip-flop mechanism of Figure 13C might occur within the complex of **1** and d-

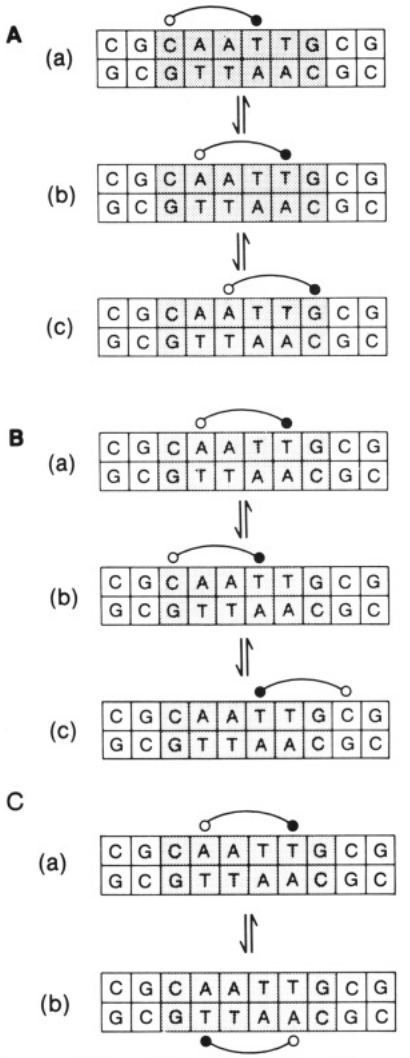

FIGURE 13: Representation of alternative types of dynamic processes in the complex formed between lexitropsin **1** and d$(CGCAATTGCG)_2$. The dissymmetric ligand is represented by two linked circles: (A) sliding motion, (B) walking process, and (C) flip-flop motion relative to the DNA.

$(CGCAATTGCG)_2$, or it might involve transient dissociation of the complex, perhaps involving exchange of drug molecules between different DNA duplexes.

Even though a definite assignment of a mechanism cannot yet be made, there is an observation that would appear to indicate an intramolecular rearrangement mechanism, without dissociation of the complex. This is the kinetic stabilization of the Watson–Crick base pairs as judged from the slow exchange of the imino protons in the complex, which indicates that the drug reduces the solvent accessibility of the imino protons of the DNA. Thus all the five imino protons of the drug–DNA complex can be observed at 21 °C, while for the free decamer all five imino proton signals can only be seen at 4 °C. A similar observation was reported by Pardi et al. (1983) for the complex between netropsin and d-$(CGCGAATTCGCG)_2$. A possible structural basis for stabilization of the labile DNA protons was proposed by Kopka et al. (1985) for a crystalline netropsin–DNA complex, i.e., that the spine of water molecules along the minor groove is displaced by the drug molecule in the complex. The rate-determining step for this two-site exchange process is the departure of the drug where it orients along the floor of the minor groove of the DNA. In an analysis of the complex of distamycin with the dodecamer d$(CGCGAATTCGCG)_2$ Klevit et al. (1986) estimated that the distamycin flips on a

DNA duplex at half the frequency at which it dissociates and estimated $k_{flip} \sim 2\ s^{-1}$ and $k_{ex} \sim 4\ s^{-1}$ at 27 °C.

CONCLUSIONS

One- and two-dimensional ^1H NMR techniques have permitted the assignment of protons in the free decadeoxyribonucleotide d(CGCAATTGCG)$_2$ and the 1:1 complex of a prototype lexitropsin, **1**, with the self-complementary decadeoxyribonucleotide. This permitted the deduction of many structural and dynamic aspects of the complex. The drug binds centrally to the decadeoxyribonucleotide in the minor groove as revealed by loss of degeneracy at these positions. Unlike the parent antibiotic netropsin, the lexitropsin is subject to significant propeller twisting about the N6–C9 bond in both the free and bound forms. The DNA in the complex exists as a right-handed helix of the B family and is very similar in its conformation to that of the free decadeoxyribonucleotide.

The drug resides on the floor of the minor groove and forms hydrogen bonds to the adenine N3 and thymine O2 positions, thus displacing the shell of hydration on the DNA. Close van der Waals contacts between the methylene protons at C15 and C16 and the A(4)·T(7) base pair may be responsible for the $(GC)_3AT$ reading of related bis(imidazole)-containing lexitropsins (Krowicki & Lown, 1987). This suggests selective and successive removal of these methylenes in further prototypes to permit reading of $(GC)_n$ sequences. Such experiments are in progress.

Exchange NMR effects permit an estimate of a rate of $\approx 44\ s^{-1}$ for the two-site exchange in the dynamic equilibrium binding of the lexitropsin with $\Delta G^{\ddagger}$ for this process estimated as $\approx 70 \pm 5$ kJ mol^{-1}. Of the alternative mechanisms considered for this exchange, the flip-flop mechanism is, at present, best in accord with the experimental observations.

These studies now provide a framework of structural information on the different factors contributing to the molecular recognition and binding of a prototype lexitropsin to DNA. They set the stage for an examination of newer lexitropsins that exhibit predictable sequence-dependent binding but no memory for the original recognition sequence of the natural products. The results of studies in this direction will be reported in due course.

Registry No. **1**, 111663-16-2; d(CGCAATTGCG), 111663-15-1.

REFERENCES

Aue, W. P., Bartholdt, E., & Ernst, R. R. (1976) *J. Chem. Phys. 71*, 2229–2246.

Berman, H. M., Neidle, S., Zimmer, C., & Thrum, H. (1979) *Biochim. Biophys. Acta 561*, 124–131.

Borah, B., Roy, S., Zon, G., & Cohen, J. S. (1985) *Biochem. Biophys. Res. Commun. 133*, 380–388.

Caruthers, M. H. (1980) *Acc. Chem. Res. 13*, 155–160.

Chazin, W. J., Wüthrich, K., Rance, M., Hyberts, S., Denny, W. A., & Leupin, W. (1986) *J. Mol. Biol. 190*, 439–453.

Frechet, D., Cheng, D. M., Kan, L. S., & Ts'o, P. O. P. (1983) *Biochemistry 22*, 5194–5200.

Frederick, C. A., Grable, J., Melia, M., Samudzi, C., Jen-Jacobson, L., Wang, B. C., Greene, P., Boyer, H. W., & Rosenberg, J. M. (1984) *Nature (London) 309*, 327–331.

Gait, M. J., Ed. (1984) *Oligonucleotide Synthesis—A Practical Approach*, IRL, Oxford.

Gronenborn, A. M., & Clore, G. M. (1985) *Prog. Nucl. Magn. Reson. Spectrosc. 17*, 1–32.

Günther, H. (1980) *NMR Spectroscopy*, pp 234–280, Wiley, New York.

Gupta, G., Sarma, M. H., & Sarma, R. H. (1984) *J. Biomol. Struct. Dyn. 1*, 1457–1472.

Gurskii, G. V., Tumanyan, V. G., Zasedatelev, A. S., Zhuze, A. L., Grokhovsky, S. L., & Gottikh, B. P. (1977) in *Nucleic Acid–Protein Recognition* (Vogel, H. J., Ed.) p 189, Academic, New York.

Hahn, F. E. (1975) in *Antibiotics III. Mechanism of Action of Antimicrobial and Antitumor Agents* (Corcoran, J. W., & Hahn, F. E., Eds.) pp 79–100, Springer-Verlag, New York.

Hare, D. R., Wemmer, D. E., Chou, S.-H., Drobny, G., & Reid, B. R. (1983) *J. Mol. Biol. 171*, 319–336.

Hore, P. J. (1983) *J. Magn. Reson. 55*, 283–300.

Kim, S. H., Sussman, J. L., & Church, G. M. (1974) *Structure and Conformation of Nucleic Acids and Protein–Nucleic Acid Interactions* (Sundaralingam, M., & Rao, S. T., Eds.) pp 571–575, University Park Press, Baltimore, MD.

Kissinger, K., Krowicki, K., Dabrowiak, J. C., & Lown, J. W. (1987) *Biochemistry 26*, 5590–5595.

Klevit, R. E., Wemmer, D. E., & Reid, B. R. (1986) *Biochemistry 25*, 3296–3303.

Kolchinskii, A. M., Mirazaabekov, A. D., Zasedatelev, A. S., Gurskii, G. V., Grokhovskii, S. L., Zhuze, A. L., & Gottikh, B. P. (1975) *Mol. Biol. (Kiev) 9*, 14.

Kopka, M. L., Yoon, C., Goodsell, D., Pjurra, P., & Dickerson, R. E. (1985) *Proc. Natl. Acad. Sci. U.S.A. 82*, 1376–1380.

Krowicki, K., & Lown, J. W. (1987) *J. Org. Chem. 52*, 3493–3501.

Le Pecq, J.-B., & Paoletti, C. (1967) *J. Mol. Biol. 27*, 87–106.

Leupin, W., Chazin, W. J., Hyberts, S., Denny, W. A., & Wüthrich, K. (1986) *Biochemistry 25*, 5902–5910.

Lown, J. W., Hanstock, C. C., Imbach, J.-L., Rayner, B., & Vasseur, J. J. (1985) *J. Biomol. Struct. Dyn. 2*, 1125–1135.

Lown, J. W., Krowicki, K., Bhat, U. G., Skorobogaty, A., Ward, B., & Dabrowiak, J. C. (1986) *Biochemistry 25*, 7408–7416.

Macura, S., & Ernst, R. R. (1980) *Mol. Phys. 41*, 95–117.

Marion, D., & Wüthrich, K. (1983) *Biochem. Biophys. Res. Commun. 113*, 967–974.

Noggle, J. H., & Schirmer, R. D. (1971) *The Nuclear Overhauser Effect: Chemical Applications*, Academic, New York.

Pardi, A., Morden, K. M., Patel, D. J., & Tinoco, I. (1983) *Biochemistry 22*, 1107–1113.

Patel, D. J. (1982) *Proc. Natl. Acad. Sci. U.S.A. 79*, 6424–6428.

Patel, D. J., Kozlowski, S. A., & Bhatt, R. (1983) *Proc. Natl. Acad. Sci. U.S.A. 80*, 3908–3912.

Patel, D. J., Shapiro, L., & Hare, D. (1986) *J. Biol. Chem. 261*, 1223–1229.

Scheek, R. M., Russo, N., Boelons, R., Kapstein, R., & van Boom, J. H. (1983) *J. Am. Chem. Soc. 105*, 2914–2916.

States, D. J., Haberkorn, R. A., & Ruben, D. J. (1982) *J. Magn. Reson. 48*, 286–292.

Sutherland, I. O. (1971) *Annu. Rep. NMR Spectrosc. 4*, 71–225.

Takeda, Y., Ohlendorf, D. H., Anderson, W. F., & Matthews, B. W. (1983) *Science (Washington, D.C.) 221*, 1020–1026.

Wartell, R. M., Larson, J. E., & Wells, R. D. (1974) *J. Biol. Chem. 249*, 6719–6731.

Zakrzewska, K., Lavery, R., & Pullman, B. (1983) *Nucleic Acids Res. 11*, 8825–8839.

Zimmer, C. (1975) *Prog. Nucleic Acid Res. Mol. Biol. 15*, 285–318.

Zimmer, C., & Wähert, U. (1986) *Prog. Biophys. Mol. Biol. 47*, 31–112.